Modeling Electron Transfer Thermodynamics in Protein Complexes: Interaction between Two Cytochromes c_3

Vitor H. Teixeira, António M. Baptista, and Cláudio M. Soares
Instituto de Tecnologia Química e Biológica, Universidade Nova de Lisboa, Oeiras, Portugal

ABSTRACT Redox protein complexes between type I and type II tetraheme cytochromes c_3 from *Desulfovibrio vulgaris* Hildenborough are here analyzed using theoretical methodologies. Various complexes were generated using rigid-body docking techniques, and the two lowest energy complexes (1 and 2) were relaxed using molecular dynamics simulations with explicit solvent and subjected to further characterization. Complex 1 corresponds to an interaction between hemes I from both cytochromes c_3. Complex 2 corresponds to an interaction between the heme IV from type I and the heme I from type II cytochrome c_3. Binding free energy calculations using molecular mechanics, Poisson-Boltzmann, and surface accessibility methods show that complex 2 is more stable than complex 1. Thermodynamic calculations on complex 2 show that complex formation induces changes in the reduction potential of both cytochromes c_3, but the changes are larger in the type I cytochrome c_3 (the largest one occurring on heme IV, of ~80 mV). These changes are sufficient to invert the global titration curves of both cytochromes, generating directionally in electron transfer from type I to type II cytochrome c_3, a phenomenon of obvious thermodynamic origin and consequences, but also with kinetic implications. The existence of processes like this occurring at complex formation may constitute a natural design of efficient redox chains.

INTRODUCTION

Protein electron transfer (ET) processes are very important for living organisms. These processes are involved in key metabolic pathways such as photosynthesis and respiration, and are also important in less-known ET pathways like sulfate reduction in the sulfate-reducing bacteria. In many cases, ET pathways involve a large and complex array of redox proteins, which can be soluble or associated to membranes. Both thermodynamic as well as kinetic control operates in these redox chains in order to bring directionality and specificity in the process.

Complexes between redox proteins are very difficult to analyze experimentally, due to their transient existence. Therefore, theoretical approaches through molecular modeling techniques can have considerable importance in elucidating the nature of these complexes and the ET processes operating at their level. The overall ET reaction begins with the formation of a complex (which may be specific or not) between the donor and the acceptor redox proteins, before actual ET takes place. The factors that control this ET are the protein association-dissociation steps, the reactant reorganization energy, the driving force and the electron transmission within the activated complex (Moore, 1996). In particular, the driving force (redox potential difference between the donor and acceptor redox protein) is one of the main factors determining the direction of the electron transfer process, being a determinant factor in the ET kinetics (Marcus and Sutin, 1985; Warshel, 1982).

Submitted July 11, 2003, and accepted for publication January 15, 2004.

Address reprint requests to Dr. Cláudio M. Soares, Tel.: 351-21-446-9610; Fax: 351-21-441-1277; E-mail: claudio@itqb.unl.pt.

0006-3495/04/05/2773/13 $2.00

Given the importance of the redox potential difference for the ET reaction to occur, a relatively large number of studies have been performed to investigate what happens upon complex formation. Some authors have suggested that after complex formation the redox potentials will be equalized, regardless of the values they had before the complex formation (Moore et al., 1986; Rees, 1985). Experimental (Burrows et al., 1991; Drepper et al., 1996; Vanderkooi and Erecinska, 1974; Zhang et al., 1996; Zhu et al., 1998) and theoretical (Soriano et al., 1997; Zhou, 1994) works are not in agreement with this equalization hypothesis, reporting that the complex formation has a smaller effect on the redox potential of the proteins than the equalization hypothesis would predict. Vanderkooi and Erecinska (1974) have studied the cytochrome-*c*–cytochrome-*c* oxidase and other complexes and observed that the redox potential of cytochrome *c* changed 30–40 mV upon complex formation. On the other hand, it was reported (Vanderkooi and Erecinska, 1974) that the complex formation between cytochrome *c* and cytochrome *c* peroxidase does not change the redox potential of cytochrome *c*. Since the redox potential of cytochrome *c* and cytochrome *c* peroxidase are 290 mV and −200 mV (Vanderkooi and Erecinska, 1974), respectively, complex formation would change the redox potential of the peroxidase by 490 mV, if the equalization hypothesis was right. Experiments with the complex formed by cytochrome *c* and cytochrome b_5 have also shown that complex formation does not change the redox potentials of the proteins (Burrows et al., 1991). More recent experimental studies with plastocyanin and photosystem I have shown that complex formation changes the redox potential of plastocyanin by 50–60 mV and that of photosystem I by ~25 mV (Drepper et al., 1996). Additionally, another experimental study, with the Rieske iron-sulfur protein in the cytochrome b_6f complex, has also shown that the redox potential of the

Rieske cluster is lowered by ~75 mV in the complex (Zhang et al., 1996). Theoretical works are also in agreement with the occurrence of redox potential shifts caused by complex formation. A theoretical study with the cytochrome-*c*–cytochrome-*c* peroxidase has shown that upon complex formation the cytochrome *c* changes the redox potential by 40 mV and the cytochrome *c* peroxidase by only 2.2 mV (Zhou, 1994). However, there are reports (Soriano et al., 1997) where theoretical studies on model complexes of plastocyanin and cytochrome *f* point to very small changes (10–20 mV) upon complex formation. In some theoretical (Zhou, 1994) as well as experimental studies (Drepper et al., 1996) where the reduction potential was determined in the two proteins of the complex, it was observed that the donor changed more significantly in its redox potential than the acceptor. Electron transfer is a rather complex phenomenon, which involves protein-protein association in a transient complex that seems to induce changes in the redox potential of the proteins.

The periplasm of sulfate-reducing bacteria is rich in redox proteins, with a large quantity and variety of cytochromes. These cytochromes can be found under various forms, varying from 1 to 16 heme groups and from monomeric to multimeric. They are involved in ET processes and some of the complexes formed between them and with other proteins have been experimentally (Magro et al., 1997; Matias et al., 1999a; Pereira et al., 1998; Pieulle et al., 1996; Valente et al., 2001) and theoretically (Matias et al., 1999b, 2001) characterized. Type I tetraheme cytochrome c_3 (c_3 I) is the biological redox partner of the periplasmic hydrogenase (Yagi et al., 1968). This cytochrome also interacts with other redox proteins, like the high-molecular-weight cytochrome (16Hcc) (Pereira et al., 1998), the nine-heme cytochrome *c* (9Hcc) (Matias et al., 1999a; Matias et al., 1999b), and the type II cytochrome c_3 (c_3 II) (Magro et al., 1997; Pieulle et al., 1996; Valente et al., 2001), mediating their reduction by hydrogenase. These studies showed that 16Hcc, 9Hcc, and even c_3 II can interact with hydrogenase, but the ET process is greatly improved in the presence of c_3 I.

The simultaneous existence of two tetraheme cytochromes c_3 in the periplasm has been demonstrated (Magro et al., 1997; Pieulle et al., 1996; Valente et al., 2001) in some sulfate-reducing bacteria. The c_3 I is the most well characterized, but recently another type was found in *Desulfovibrio africanus* (*Da*) (Magro et al., 1997; Pieulle et al., 1996) (where it was named acidic cytochrome c_3) and in *Desulfovibrio vulgaris* Hildenborough, i.e., *Dv*H (Valente et al., 2001) (where it was named type II cytochrome c_3, this being the nomenclature followed in this work). These two proteins are very similar in fold (Brennan et al., 2000; Czjzek et al., 1994; Einsle et al., 2001; Harada et al., 2002; Haser et al., 1979; Higuchi et al., 1984; Matias et al., 1993, 1996; Messias et al., 1998; Morais et al., 1995; Norager et al., 1999; Simões et al., 1998) and have four *c*-type hemes covalently bound with cysteine residues to one polypeptide chain of similar size. Besides these similarities these two cytochromes are different in some aspects. One of these differences is the distribution and quantity of acidic and basic residues. The c_3 I has a characteristic positive patch around heme IV (Brennan et al., 2000; Czjzek et al., 1994; Einsle et al., 2001; Harada et al., 2002; Haser et al., 1979; Higuchi et al., 1984; Matias et al., 1993, 1996; Messias et al., 1998; Morais et al., 1995; Simões et al., 1998) and a neutral region around heme I. In contrast, c_3 II has a markedly less positive surface around heme IV, and a negative zone in the region of heme I (Norager et al., 1999; Valente et al., 2001). Additionally the shorter N-terminal of c_3 II causes a higher exposure of heme I in c_3 II (Norager et al., 1999). In c_3 I there is an α-helix which is interrupted by a loop that does not exist in the c_3 II. The surface characteristics can be very important for their ET function, and may indicate different redox partners.

Redox proteins can show a marked dependence between reduction and pH, or protonation effects, and this phenomenon has been named the redox-Bohr effect (Papa et al., 1979; Xavier, 1985). It consists of an interdependence between the electronic and protonic captures, which results from electrostatic interactions between redox and protonatable groups. The midpoint redox potentials of the redox groups depend on pH, and in the same way the pK_a values of protonatable groups are influenced by the redox potential. This concerted electron and proton capture should occur in all redox proteins at some values of pH, but in some it occurs at physiological pH, making the phenomenon biologically relevant. One of the most studied examples are the tetraheme cytochromes c_3, with a large number of experimental (Coletta et al., 1991; Gayda et al., 1988; Louro et al., 2001a,b, 1997, 1996, 1998; Pereira et al., 2002; Salgueiro et al., 1997; Santos et al., 1984; Saraiva et al., 1998; Turner et al., 1994, 1996) and theoretical (Baptista et al., 1999; Martel et al., 1999; Soares et al., 1997; Teixeira et al., 2002) works. The physiological importance of the redox-Bohr effect in these cytochromes may consist of a mechanism for simultaneously capturing electrons and protons from hydrogen oxidation by hydrogenase (Louro et al., 1997) or, alternatively, it may consist of a mechanism for modulating the redox potential of groups, by using nearby protonations as a controlling factor. Whatever its biological role, it is clearly important to characterize this effect and have models that treat it correctly (Baptista et al., 1999), in order to model the redox thermodynamics of this type of cytochromes.

This work has two main objectives. The first is to characterize, at the molecular level, the modes of interaction between c_3 I and c_3 II from *Dv*H. The second is to study, using this case as an example, what happens to the thermodynamic characteristics of individual redox groups when two proteins get into contact, with the aim of understanding directionality of electron transfer in biological ET chains.

MATERIAL AND METHODS

Preparation of structures

For the cytochrome c_3 I, the structure corresponding to molecule A in the PDB entry 2CTH (Matias et al., 1993) was chosen. Since there is no three-dimensional structure determined for the cytochrome c_3 II from *Dv*H, we built a comparative model based on its sequence (retrieved from the genome sequence of this organism, available at *http://www.tigr.org*) and the structure of the cytochrome c_3 II from *Da* (Norager et al., 1999).

The c_3 II from *Da* shows 45% sequence identity with the corresponding sequence from *Dv*H. In the family of cytochromes c_3 (of type I, given that only one structure exists for type II), consisting of highly structurally conserved proteins, this sequence identity can be considered quite high, given that the average sequence identity within this family is ~40% (HOMSTRAD classification; Mizuguchi et al., 1998). This makes us confident that a good structural model can be derived (Martí-Renom et al., 2000; Sánchez and Sali, 1997). In addition, 68% of the nonconserved residues between the *D. africanus* and *D. vulgaris* sequences are located in loops. The program MODELLER (Sali and Blundell, 1993), Version 6.0, was used for deriving the structure. The alignment was optimized until a good quality model for the unknown structure was achieved. A Ramachandran analysis of the final model was performed using PROCHECK (Laskowski et al., 1993). The final structure has 85.9% of the residues in the most favored regions, and 14.1% in additional allowed regions, which is better than the statistics from the x-ray structure used as the basis for this comparative modeling, that displayed 85.1% of residues in most favored regions and 14.9% of residues in additional allowed regions. Ten internal water molecules that are conserved in this family of cytochromes were also modeled.

The selection of water molecules to include in all types of calculations presented here was done on basis of their relative accessibility; if the relative accessibility was $<10\%$, as computed with the program ASC v2.14 (Eisenhaber and Argos, 1993; Eisenhaber et al., 1995), they were included. The number of water molecules used in each of the cases is described in the first part of Results and Discussion.

Reduction and protonation thermodynamics

The joint binding equilibrium of protons and electrons was studied with a combination of continuum electrostatics (CE) and Monte Carlo (MC) methods. This followed a procedure already described in previous works (Baptista and Soares, 2001; Teixeira et al., 2002), where details not reported here can be found. The CE calculations were performed with MEAD v2.2.0 (Bashford, 1997; Bashford and Gerwert, 1992) using the GROMOS96 charge set (Scott et al., 1999) for the atomic charges of normal residues, and using previously determined charges (Martel et al., 1999) for the heme and attachment groups. The MC sampling was done with the PETIT program (Baptista et al., 1999; Baptista and Soares, 2001). In the CE calculations the final grid dimensions used were $90 \times 90 \times 90$ Å for the individual proteins and $100 \times 100 \times 100$ Å for the complexes. The simulations were done at pH 7.0 and the electrostatic potential was scanned in steps of 10 mV, from -700 to 50 mV in the individual proteins, and -700 to 300 mV in the complexes. The dielectric constant used in the CE calculations for the protein was 20 and for the solvent was 80 (see Baptista and Soares, 2001, and Teixeira et al., 2002, for a discussion of these values).

Molecular dynamics simulations

The molecular mechanics/dynamics simulations were performed with the GROMOS96 package (Scott et al., 1999; van Gunsteren et al., 1996). The heme energy functions were modified in a similar way as specified in Soares et al. (1998), to treat the *c*-type hemes present in these cytochromes. The atomic partial charges used were the ones specified in the previous section. The protons were added to the protein considering their predominant protonation state at pH 7.0, determined by the CE/MC methods described in the previous section. The calculations were performed assuming the fully oxidized state for the two cytochromes.

The systems were solvated in truncated octahedron boxes originated from cubes with sizes of 71.989 Å/side for the individual proteins, 88.224 Å/side for complex 1, and 94.139 Å/side for complex 2, generated by replication of an initial equilibrated box of water at the experimental density at 300 K and 1 bar (constant temperature and volume). The SPC water model (Hermans et al., 1984) was used in the calculations. The final systems had 5560 waters for c_3 I, 5604 waters for c_3 II, 10,254 waters for complex 1, and 12,693 waters for complex 2. The hydrogen atom positions were optimized using energy minimization in two stages, the first one consisting in 5000 steps with the steepest-descent method, and the second consisting in 5000 steps with the steepest-descent method and with SHAKE (Ryckaert et al., 1977) constraints in all bonds. A 10^5 kJ/(mol nm) position-restraining force constant was used in all heavy atoms in these two minimization steps.

The molecular dynamics simulations were performed using heat baths (Berendsen et al., 1984) at 300 K, with separate coupling for the solvent and solute, and using, unless otherwise stated, coupling constants of 0.1 ps. SHAKE (Ryckaert et al., 1977) was used in all bonds, with a geometric tolerance of 0.0001. The equations of motion were integrated using a time step of 0.002 ps. Nonbonded interactions were treated with the twin-range method (van Gunsteren and Berendsen, 1990), using group-based cutoffs of 8 and 14 Å, updated every 10 steps. The electrostatic forces thus truncated were corrected with forces corresponding to a continuum reaction field (Barker and Watts, 1973; Tironi et al., 1995) using a dielectric constant of 54, the dielectric constant of SPC water under these circumstances (Smith and Honig, 1994).

The initialization of each MD run was done in two steps. The first step consisted of a 50-ps simulation with all protein atoms position restrained with a 10^5 kJ/(mol nm) force constant with initial velocities taken from a Maxwell-Boltzmann distribution at 300 K and a temperature-coupling constant of 0.01 ps. The second step consisted of a 50-ps simulation at the same temperature with a temperature-coupling constant of 0.1 ps and the positions of all Cα atoms restrained with a force constant of 10^5 kJ/(mol nm).

Rigid-docking calculations

The interaction between the tetraheme cytochromes c_3 was studied using AUTODOCK v2.4 (Goodsell et al., 1993; Goodsell and Olson, 1990). The atomic charges were those already used above. The general methodology for this kind of interaction study can be found in previous works (Cunha et al., 1999; Matias et al., 1999b, 2001). The calculations were done assuming the fully oxidized state for the two cytochromes. The protonation states of all residues were the predominant ones calculated previously by CE/MC, at pH 7.0.

Two grids were used in the calculations and they were positioned in a way that ensured covering of all the interaction space between the two proteins. The search for low energy solutions was performed using 400 runs of MC simulated annealing in translational and rotational space. Each run consisted in 100 cycles of MC at progressively lower temperature. The initial temperature of each cycle and temperature reduction factor per cycle were chosen in a way that ensured a large acceptance/rejection ratio in the beginning and a low acceptance/rejection ratio at the end. In this case we used a RT value of 146 kJ/mol with a temperature reduction factor per cycle of 0.94. The initial translation step was 1.0 Å and the initial quaternion rotational step was 30°. Reduction factors of 0.9702 and 0.9770 per cycle were used for the maximum translation and rotational steps, respectively, which resulted in 0.05 Å maximum translation steps and 3° maximum rotation steps in the last cycle. This procedure gives a large number of solutions, which are ranked according to their energy and their root mean-square deviation (RMSD). Each rank can have one or more solutions.

Binding free energy

The binding free energy of two interacting proteins was calculated in a way similar to the one described earlier by other authors (Froloff et al., 1997; Kuhn and Kollman, 2000), and can be written as

$$\Delta G_b = G_{complex} - (G_{protein1} + G_{protein2}), \quad (1)$$

in which G_x (x standing for the complex or for the individual proteins) is defined as

$$G_x = G_{el} + G_{np} + G_{strain} - TS_{mc} - TS_{sc} - TS_{r,t}. \quad (2)$$

The G_{el} and G_{np} terms are the electrostatic and nonpolar contributions, respectively. G_{strain} accounts for molecular mechanics non-electrostatic terms. TS_{mc} and TS_{sc} describe the configurational entropy of the main-chain and side-chain torsional freedom. $TS_{r,t}$ accounts for the translational and rotational degrees of freedom. TS_{mc} is not considered here, because it depends on the length of the chain, and since the number of residues is the same before and after complex formation, these terms will likely cancel. The $TS_{r,t}$ term is also not considered here, because it is approximately the same for a set of similar configurations, and this effect on the relative binding free energy should be very small (Gilson et al., 1997).

The electrostatic term was calculated as a sum of Coulombic and solvation terms (Froloff et al., 1997; Gilson and Honig, 1988; Smith and Honig, 1994),

$$G_{el}(\varepsilon_i, \varepsilon_0) = G_{coul}(\varepsilon_i) + G_{solv}(\varepsilon_i, \varepsilon_0), \quad (3)$$

where ε_i and ε_0 are the dielectric constants for the protein and for the solvent, respectively. The Coulombic term was calculated with GROMOS96 (Scott et al., 1999; van Gunsteren et al., 1996) using a dielectric constant of 2 for the protein (Froloff et al., 1997; Gilson and Honig, 1988). The electrostatic solvation term, G_{solv}, was calculated with the finite difference Poisson-Boltzmann method as implemented in the MEAD package (Bashford, 1997; Bashford and Gerwert, 1992). The atomic charges and radii were the ones already described above. The grid sizes were chosen in a way that ensures that all the protein is enclosed. We used an initial grid with 90 Å per side with grid spacing of 1 Å followed by a focusing calculation with a grid of 55 Å per side and grid spacing of 0.25 Å. With the exceptions of the ionic strength, which was set to 0, and the dielectric constant of the protein interior, which was considered 2, the other parameters are the same as described above. We used this dielectric constant to account for electronic polarizability. Higher values are generally used to account for the dielectric response due to configurational changes, but these are treated in the G_{strain} term.

The nonpolar (hydrophobic) contribution to the binding free energy, G_{np}, was calculated as described in Sitkoff et al. (1994), using a term $G_{np} = \gamma\, SA + b$ for each molecule, where SA is the solvent-accessible surface area, here calculated with the program ASC v2.14 (Eisenhaber and Argos, 1993; Eisenhaber et al., 1995), and γ and b are constants with the values 0.005 kcal/(mol Å^2) and 0.860 kcal/mol, respectively.

The G_{strain} term includes the bonded (bond, bond-angle, and torsional angles) and the van der Waals energy, which is calculated by molecular mechanics using GROMOS96 (Scott et al., 1999; van Gunsteren et al., 1996).

The TS_{sc} term is calculated using the empirical scale of Pickett and Sternberg (1993), which only considers the residues with relative accessibility (RA—here calculated with ASC v2.14; Eisenhaber and Argos, 1993; Eisenhaber et al., 1995) >60%. The accessibility is calculated relative to a tripeptide Ala-X-Ala, with the following angles: $\phi = -140°$, $\psi = 135°$, $\omega = 180°$, $\chi_1 = -120°$, and the other side-chain dihedrals set to 180° (Chothia, 1976). The entropic term is obtained summing all entropic contributions of the residues with RA > 60%, using the rotamer empirical base of Pickett and Sternberg (1993).

RESULTS AND DISCUSSION

General modeling approach

The x-ray structure of c_3 I and the comparative model of c_3 II were analyzed by CE/MC to determine their predominant protonation states at pH 7.0. This calculation was performed with 14 water molecules for c_3 I and 7 for c_3 II. A 4-ns MD simulation in water was then performed for the two types of cytochromes, including those water molecules and using the determined predominant protonation states. Average structures of the last 2 ns (from 2 to 4 ns) were calculated. These average structures included the internal water molecules that were always inside the protein in the considered time period (the same water molecule), and were the starting point for the rigid-body docking simulations. The two lowest energy complexes from the docking simulations were selected and relaxed by MD for 2 ns in water. The relative stability of these two different configurations was estimated using the binding free energy procedure describe above. For doing this, 20 structures taken from the MD simulation of the isolated proteins (corresponding to the 2–4-ns period) and 10 structures taken from the simulation of the complexes (corresponding to the 1–2-ns period) were used. These structures were sampled at 100-ps intervals, and no water molecules were considered. The binding free energy of each of the complexes was calculated as an arithmetic average and also as a sum-over-states of the form $G = -RT \ln \Sigma_c \exp(-G(c)/RT)$, where $G(c)$ is the free energy of each conformation c. The same structures used in the binding free energy calculation were also used in the CE/MC calculation, but in this case the internal water molecules were included: 8 for c_3 I, 3 for c_3 II, 22 for complex 1, and 21 water molecules for complex 2. The titration curves of each individual structure were used to obtain an arithmetic average curve for the individual cytochromes and complexes. These average curves and their associated values (e.g., midpoint potentials) are the subject of the analysis. In this work we made the approximation of considering only simulated oxidized structures in the thermodynamic calculations. A similar approximation of using oxidized x-ray structures has been used before with considerable success to study similar phenomena in diverse cytochromes c_3 (Baptista et al., 1999; Martel et al., 1999; Soares et al., 1997; Teixeira et al., 2002). Recently (Bento et al., 2004, 2003; Louro et al., 2001a), we have used fully oxidized and fully reduced x-ray structures to understand cooperativity phenomena in cytochrome c_3 and on the nine-heme cytochrome c and found small differences in the global redox potentials calculated with structures at different oxidation states. Despite being important for explaining the cooperativity phenomena, these differences are small, of ~2 mV for the case of cytochrome c_3 from D.

desulfuricans ATCC27774 (the most relevant case for the present work) and 5 mV for the case of the nine-heme cytochrome *c* from the same organism. The present work could have used simulated oxidized and reduced structures of the system (e.g., like in Bret et al., 2002) as input for doing the thermodynamic calculations, but, besides doubling the computational needs, this approach would increase the complexity of the required treatment and would introduce new sources of uncertainty. Therefore we decided to focus ourselves on the problem of complex formation and its consequences, bearing in mind that a small error (whose best estimate available would be ~2 mV) may be introduced by the use of oxidized conformations only.

Protein-protein interaction studies by rigid docking

As discussed in the Introduction, kinetic experiments showed that the reduction of c_3 II by hydrogenase is faster in the presence of catalytic amounts of c_3 I (Valente et al., 2001), which suggest an interaction between c_3 I and c_3 II. Therefore, our first objective was to determine possible interaction solutions for these two proteins.

The clustering of all solutions of the molecular interaction between c_3 I and c_3 II is shown in Fig. 1 *A*. The regions around heme I and heme IV of c_3 I are the most populated, followed by the region of heme III. Heme II of c_3 I is clearly not a favorable site of interaction with c_3 II, showing a very small number of possible solutions. We can invert Fig. 1 *A*, fitting all possible solutions of c_3 II, in a way that c_3 I will be positioned around c_3 II (Fig. 1 *B*). The solutions presented in Fig. 1 *B* are the same as the ones presented in Fig. 1 *A*, but here we can look at the most interesting zones of c_3 II that interact with c_3 I. The most populated zones of c_3 II that interact with c_3 I are around heme I and III. The region around heme II shows almost no interaction with c_3 I, and the zone of heme IV has a small number of solutions. From all these interaction solutions, we selected the two most probable ones, which are represented in Fig. 1 *C* and *D*. The lowest energy complex (complex 1), which corresponds to an interaction energy of −61.75 kcal/mol and 35 solutions, is represented in Fig. 1 *C*. Complex 1 corresponds to an interaction between heme I from c_3 I with heme I from c_3 II. The second lowest energy solution (complex 2), which corresponds to an interaction energy of −59.81 kcal/mol and 18 solutions, is represented in Fig. 1 *D*. Complex 2 corresponds to the interaction between heme IV from c_3 I with heme I from c_3 II.

It is surprising to find that the lowest energy complex does not correspond to an interaction involving the zone of heme IV from c_3 I. In fact, this is the zone evidenced by other studies (Matias et al., 1999b, 2001) to be the one in contact with its physiological partners. This zone contains a lysine patch (Brennan et al., 2000; Czjzek et al., 1994; Einsle et al.,

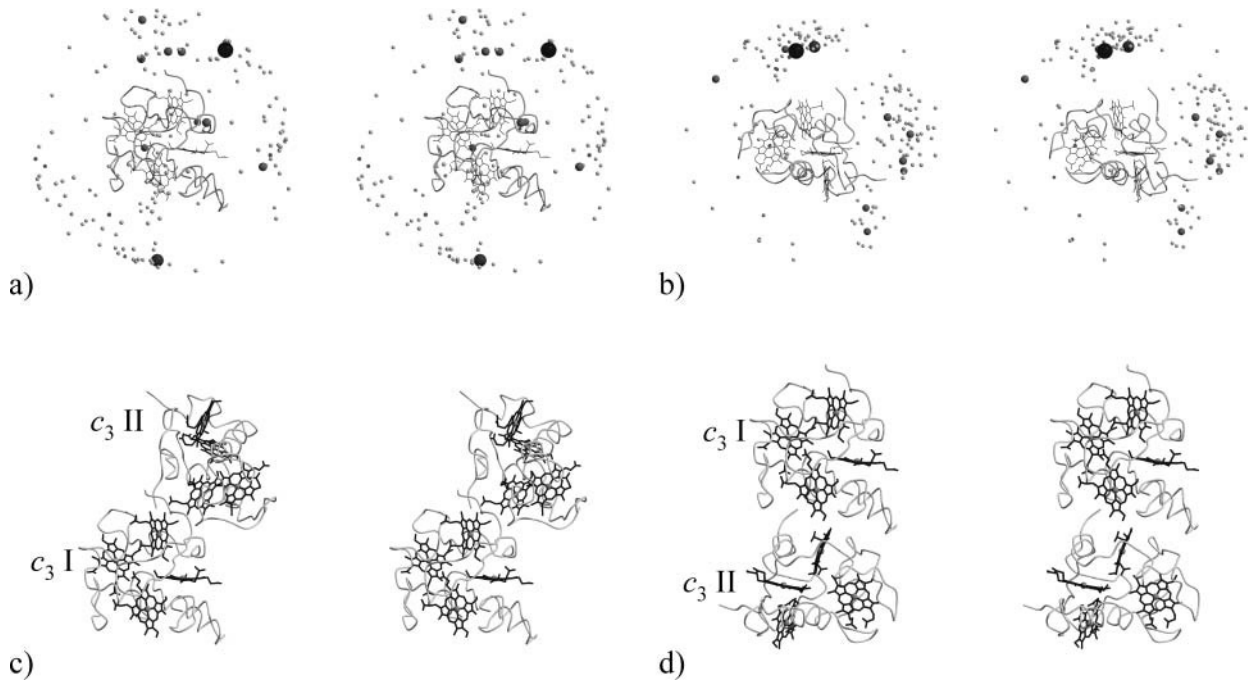

FIGURE 1 Rigid-docking results of the interaction between c_3 I and c_3 II from *Dv*H. (*A*) Stereo representation of the center of geometry of all interaction (clustered) solutions or ranks of c_3 II represented as spheres, the c_3 I as main fold, and the hemes as sticks. Larger and darker spheres correspond to lower energy solutions. (*B*) Same as *A*, but in this case the c_3 I solutions are represented as spheres, whereas the c_3 II is represented as main fold with its hemes as sticks. (*C*) Stereo representation of complex 1, with both cytochromes represented as their main fold and hemes as sticks. (*D*) same as *C*, but for complex 2. Figures were prepared using MolScript (Kraulis, 1991) and Raster3D (Merrit and Bacon, 1997).

2001; Harada et al., 2002; Haser et al., 1979; Higuchi et al., 1984; Matias et al., 1993, 1996; Messias et al., 1998; Morais et al., 1995; Simões et al., 1998), which is supposed to be involved in the interaction with negatively charged zones of protein partners. The interaction between this lysine patch and a negatively charged zone of c_3 II is only found in complex 2, which differs by <2 kcal/mol from complex 1. Given the large approximations imposed by rigid-docking methods, we decided to analyze further both lowest energy complexes, using more sophisticated approaches. In any case, it is worth noting that complex 1 corresponds to an interaction topology that is observed in the octaheme cytochromes c_3 (or dimeric cytochrome c_3) (Czjzek et al., 1996; Frazão et al., 1999), where the hemes I from the two molecules constituting the dimer are brought into contact.

Relaxation of the protein complexes using MD simulations

The rigid-body docking procedure used in this study can be seen as an initial approximation. To simulate the close interaction of the two proteins in complex, and particularly the interface, we need to introduce flexibility into the models. One way to do this is to perform MD simulation of the complex. Here we performed, for complexes 1 and 2, MD simulations using explicit solvent, spanning a period of 2 ns.

Fig. 2, *A–D*, shows the RMSD of the C_α atoms during the MD simulations of the individual cytochromes and of complexes 1 and 2. The values of RMSD obtained are within reasonable values, mostly for the free proteins, showing that the simulations are sufficiently stabilized, with just small drifts. Comparison between the time evolution of the RMSD and final values reached in the MD simulations of the two isolated proteins evidences similar behavior for both MD simulations starting from the x ray of type I cytochrome c_3 (Fig. *2 A*); and for the one starting from the comparative model of the type II cytochrome c_3 derived here (Fig. *2 B*), with type II showing only a slightly higher value of RMSD, which is within reasonable values for this type of MD simulation. This observation makes us more confident on the quality of the comparative model of the type II cytochrome c_3, given that, in our experience, less-optimum comparative models usually present higher values of RMSD in similar procedures. Although the RMSD of the complex 2 seems to be slightly high compared to that of complex 1, the RMSD of the individual proteins in complex 2 is systematically low (data not shown). This means that this higher RMSD is due to relative rigid-body displacement of both cytochromes in this complex.

Each complex structure was averaged in the 1–2-ns period, and compared with the 2–4-ns average structures of the individual cytochromes, obtained from the simulations of the individual proteins. This comparison is presented in Fig. 3, *A*

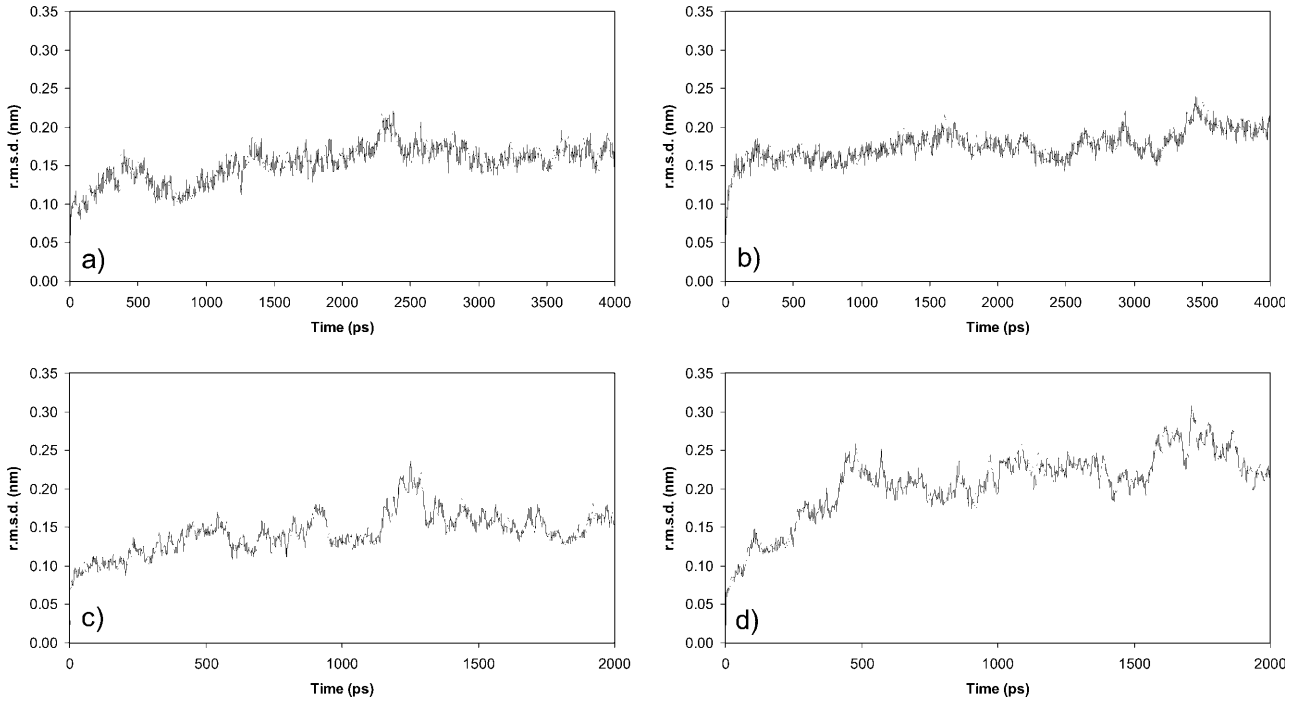

FIGURE 2 Structural analysis of the molecular dynamics simulations in water. RMSD (from initial conformation) of the C_α atoms in the 4-ns MD simulations starting from the x-ray structure of c_3 I (*A*) and the comparative model structure of c_3 II (*B*). RMSD (from initial conformation) of C_α atoms in the 2-ns simulations starting from complex 1 (*C*) and from complex 2 (*D*), which resulted from the rigid-docking simulation.

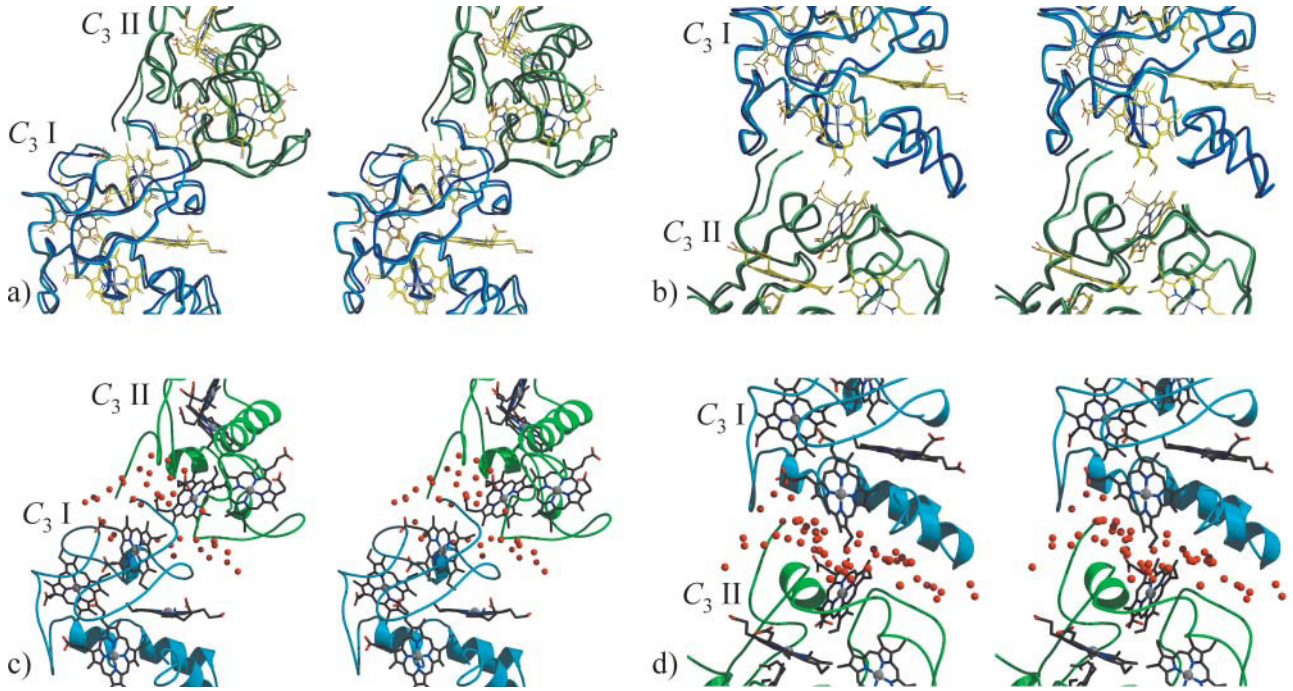

FIGURE 3 Stereo pictures comparing free and bound cytochromes structures for complex 1 (*A*) and complex 2 (*B*). The rigid-docking structures (corresponding to the 2-ns conformation of the free cytochromes simulations in water) are colored in light blue for c_3 I and light green for c_3 II, whereas the corresponding cytochrome structures after the 2-ns simulations of the complexes are dark blue and dark green, respectively. Hemes are represented with sticks. *C* and *D* represent the final structures of the complex 1 and 2 simulations, respectively, with interface water molecules represented as red spheres. The same color-coding of *A* and *B* is used in *C* and *D*. Figures were prepared using MolScript (Kraulis, 1991) and Raster3D (Merrit and Bacon, 1997).

and *B*, where the changes induced in the main chain of both cytochromes by the formation of each complex can be appreciated. These changes are small in both complexes, especially in complex 2.

The number of electrostatic contacts in the two complexes is the same (Table 1). The relatively small number of electrostatic contacts, when compared with previous studies (Cunha et al., 1999; Matias et al., 1999b, 2001) may lie on the fact that, contrary to these other studies, in the present case the relaxation of the complexes was made with explicit solvent, which originates weaker electrostatic interactions. Despite this similarity in the number of electrostatic contacts, electrostatic interactions within the two complexes show a significant difference; the total electrostatic energy from the PB/SA procedure (see below) of going from the free molecules to the complex is 30.2 kcal/mol for complex 1 and −22.8 kcal/mol for complex 2, evidencing more favorable interactions in the latter.

Both permanent as well as transient interface water molecules (within 4 Å from both cytochromes simultaneously) were calculated and the results show (Table 1) that the interface of complex 2 has a slightly higher number of water molecules (15% and 23% more for permanent and transient water molecules, respectively). More importantly, the water distribution at the interfaces is different. In the interface of complex 2, the arrangement of the water molecules between the two cytochromes seems to form a water layer (Fig. 3 *D*), which is not present in complex 1 (Fig. 3 *C*). Additionally, the contact surface calculated for complex 1 is larger than that from complex 2, contrary to one might think when looking at Fig. 1, *C* and *D*. This lower contact surface of complex 2 may be due to the water layer at the interface of the complex. All these data point to a structuring role of water at the interface of these complexes (mostly complex 2), even if part of this water is transient (almost 40% in the case of complex 2). Interestingly, the substantial fluctuation in the number of transient water molecules (Table 1), shows the complex interface to be rather dynamic.

The binding free energy calculations used here can be considered better estimates of the actual binding energy between the two proteins in different interaction configurations than the rigid-body docking energies. This is because they are performed on a set of relaxed structures in a natural solvated environment and they contain better electrostatic energy estimates, in addition to other energy and entropy terms not contained in the rigid-body docking energies. These binding free energy calculations, performed for the two complexes, are here used as qualitative estimates of their relative stability. According to these calculations, complex 2 appears to be more stable than complex 1, with −74.0 kcal/mol and −24.6 kcal/mol, respectively, obtained from an arithmetic average over all sampled conformers within the equilibrate period of the trajectories—i.e., the final

TABLE 1 Comparative analysis of the two complexes

		Complex 1	Complex 2
Contact surface*		1494 Å^2	1085 Å^2
Number of interface waters†	Permanent	35	41
	All	44 ± 7	57 ± 11
Favorable electrostatic contacts‡		NT-PrAI	K57-E29
		K3-PrDI	K60-D3
		K3-PrAI	K60-D25
		K26-D53	D71-NT
		K29-E55	K72-PrAI
		E41-NT	K94-E55
		E41-R1	K101-E34
Electrostatic energy§		30.2 kcal/mol	−22.8 kcal/mol
Binding free energy (average)		−24.6 kcal/mol	−74.0 kcal/mol
Binding free energy (sum-over-states)		4.8 kcal/mol	−81.8 kcal/mol

All of the calculations and analyses below were made on the equilibrated part of the MD simulations, i.e., the final 2 ns (2–4-ns period) for isolated proteins and the final 1 ns (1–2-ns period) for the complexes.
*(Surface of Protein 1 + Surface of Protein 2) − Surface of Complex.
†Waters lying within 4 Å of both proteins in a permanent or transient manner (all = permanent + transient). Fluctuations are shown as ±2 SD.
‡Interface salt-bridges which occur >50% of the time in the selected period of the MD simulations (c_3 I–c_3 II).
§(Coulomb + Solvation Energies of the Complex) − (Sum of Coulomb + Solvation Energies of the Free Proteins).

2 ns (2–4-ns period) in the case of isolated proteins and the final 1 ns (1–2-ns period) in the case of the complexes. Furthermore, a sum-over-states, which accounts for the entropy of the set of conformers, gives comparable results, with −81.8 kcal/mol and 4.8 kcal/mol for complexes 2 and 1, respectively. Therefore, despite what was found by rigid docking, complex 2, according to these more sophisticated approaches, seems to be a more favorable interaction solution. These evidences show again the importance of heme IV and the lysine patch zone of c_3 I in the interaction with its partners. In view of this result, and unless otherwise stated, we will continue our analysis and discussion using complex 2.

Reduction and protonation thermodynamics

The electron transfer from c_3 I to c_3 II has already been experimentally demonstrated by kinetic methods (Valente et al., 2001). Here we will briefly analyze the ET from the thermodynamic point of view, using theoretical methodologies. Besides analyzing ET in the individual proteins, we will also analyze what happens to the proteins when associated. This is a very important question, with thermodynamic but also with kinetic implications, given that the free energy for ET (or driving force) is an important component in the kinetics of ET processes (Marcus and Sutin, 1985). Any changes from the free protein situation will likely have physical and physiological implications.

As mentioned in the Introduction, before the ET occurs, a complex has to be formed between the two redox proteins, the donor and the acceptor. The nature of this process has been the subject of several proposals. Some authors suggest that the redox potential difference between the donor and acceptor will be equalized after formation of the complex (Moore et al., 1986; Rees, 1985). However, an experimental work with cytochrome *c* and various redox proteins disagrees with this suggestion and demonstrated that complex formation has smaller effects on the redox potential of the redox proteins (Vanderkooi and Erecinska, 1974). More recent experimental (Drepper et al., 1996; Zhang et al., 1996; Zhu et al., 1998) and theoretical (Soriano et al., 1997; Zhou, 1994) works are in agreement with Vanderkooi and Erecinska (1974), showing that the redox potential changes after complex formation are smaller than what the equalization hypothesis would require, and some also show that the changes in redox potential are more pronounced in the donor than in the receptor redox protein (Drepper et al., 1996; Zhou, 1994; Zhu et al., 1998), increasing the ET driving force.

Fig. 4, *A* and *B*, contains the global redox titration curves of c_3 I and c_3 II, respectively, in the free and bound states. We can see that complex formation induces a shift toward more negative potentials in the redox titration of the c_3 I. In contrast, the c_3 II has a much smaller decrease. It is worth noting that, after complex formation, the redox potential of the two cytochromes experiences a different decrease (Fig. 4, *A* and *B*). The c_3 I decreases its redox potential by ~36 mV and the c_3 II by only ~5 mV. These plots show that the interaction between proteins can cause noticeable changes in their redox potentials. The magnitude of the changes observed in this work is comparable to those reported for complexes involving other redox proteins (Drepper et al., 1996; Vanderkooi and Erecinska, 1974; Zhang et al., 1996; Zhou, 1994; Zhu et al., 1998). Furthermore, this shows that the redox partner experiencing a larger potential shift upon complex formation is the donor, as previously observed (Drepper et al., 1996; Zhou, 1994; Zhu et al., 1998).

Rearranging the data contained in plots *A* and *B* of Fig. 4, to analyze both cytochromes in the same plot, we get Fig. 4, *C* and *D*, where the free and bound situation is characterized. This allows us to evidence a very important result of this study, which is the inversion of the titration curves from the free to the complex form. In the free form (Fig. 4 *C*), as judged from its higher redox potential (Table 2), c_3 I has no propensity to transfer electrons to c_3 II, suggesting that the ET reaction as a whole would not be very efficient in this direction (the experimentally observed one), both from the thermodynamic as well as the kinetic point of view. However, when the two proteins get together, the redox potential of c_3 I becomes lower than that of c_3 II (Table 2), favoring the transfer of electrons from the former to the latter. In conclusion, complex formation transformed an initially unfavorable ET reaction into one that is favorable (Fig. 4, *C* and *D*), following the proposed direction of electron transfer (Valente et al., 2001).

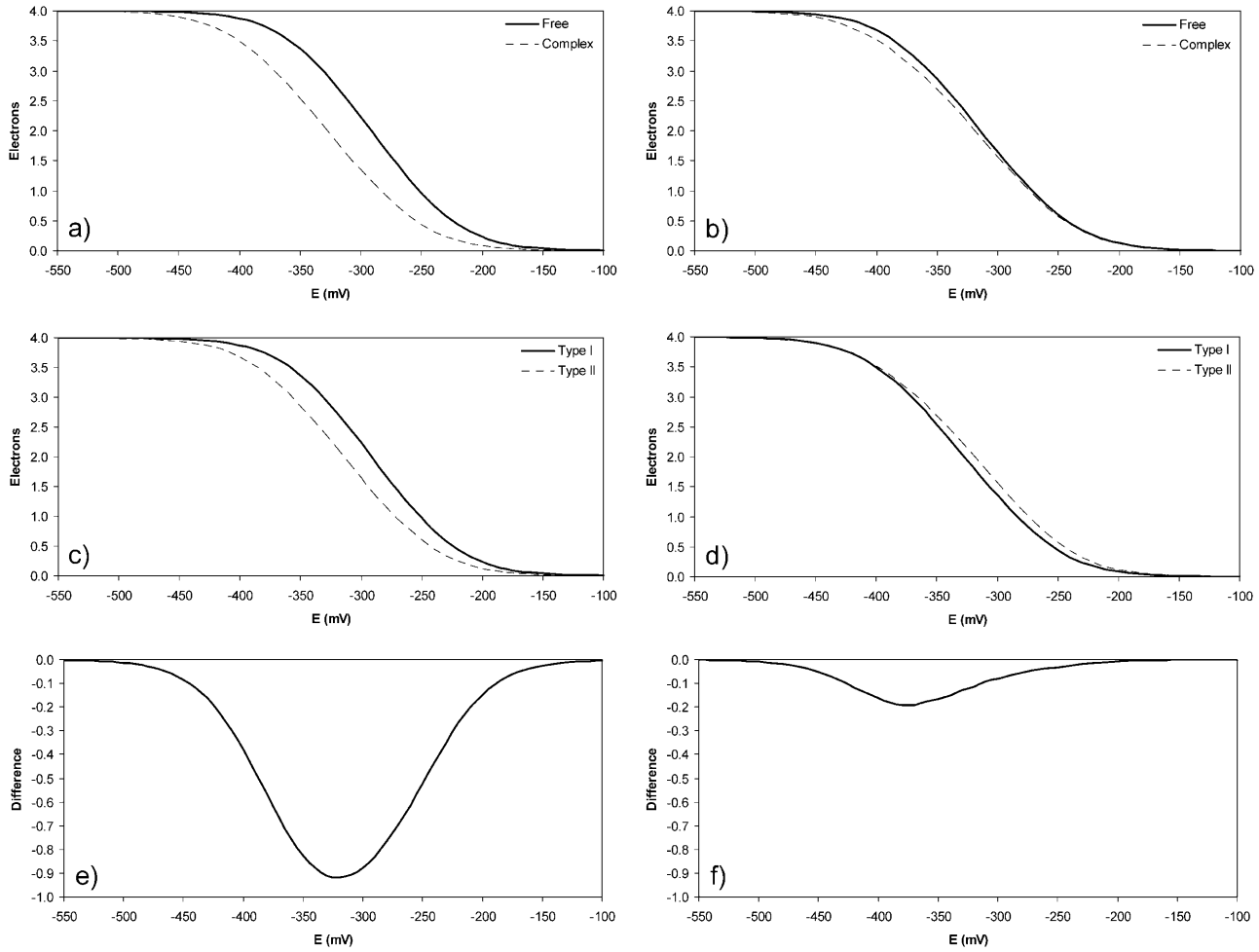

FIGURE 4 Global redox titration curves of the cytochromes c_3 at pH 7.0. Titration curves of c_3 I (*A*) and c_3 II (*B*) in the free (*solid line*) and complex 2 (*dashed line*) forms. Titration curves of c_3 I (*solid line*) and c_3 II (*dashed line*), in the free (*C*) and complex 2 (*D*) forms. Difference between the complex 2 and the free forms (complex-free) in c_3 I (*E*) and c_3 II (*F*), respectively. These calculations were made using conformations taken from the equilibrated part of the MD simulations, namely the final 2 ns (2–4-ns period) in the case of isolated proteins and the final 1 ns (1–2-ns period) in the case of the complexes.

If we compute the difference between the titration curves of each cytochrome c_3 when in complex and in free forms (Fig. 4, *E* and *F*), we can clearly see how the changes vary along the titration. These difference curves show that there is a region, around the protein midpoint titration (~ -330 mV), in which c_3 I has approximately one electron less in the complex form than in the free form. The c_3 II only presents small differences between the complex and the free form. This may be interpreted as considering that complex formation generates a thermodynamic release of an electron in c_3 I, meaning that c_3 I loses affinity for the electrons after formation of the complex.

Despite having considered complex 1 as a less likely interaction solution, we can perform on it the same thermodynamic analysis used for complex 2. We find that complex formation in this case does not change the order of the reduction curves (not shown), as can also be seen from the redox potentials on Table 2. Thus complex 1 evidences no propensity for electron transfer in the direction observed experimentally.

The variation, upon complex formation, of the individual heme redox potentials in the two types of cytochromes can also reveal some interesting results. Fig. 5 shows the protein and heme redox potential of the two cytochromes in the free and complex 2 forms. The changes upon complex formation are clearly visible, with the hemes from c_3 I (Fig. 5 *A*) undergoing larger changes than the hemes from c_3 II (Fig. 5 *B*). With the exception of heme I from c_3 I, all its heme redox potentials change at least 30 mV, with heme IV experiencing

TABLE 2 Protein midpoint redox potentials

	c_3 I	c_3 II
Free	−291	−314
Complex 1	−300	−315
Complex 2	−327	−319

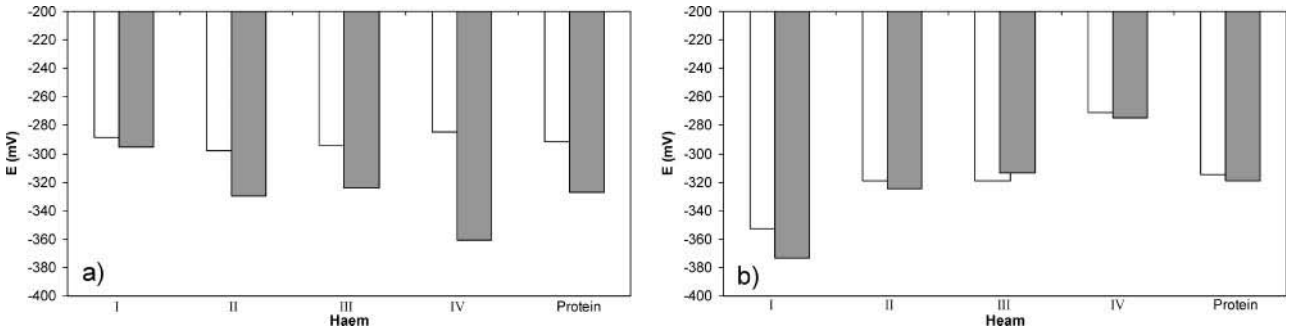

FIGURE 5 Heme and protein midpoint redox potential changes in (*A*) c_3 I and (*B*) c_3 II upon formation of complex 2 at pH 7.0. Open bars correspond to the free form, whereas the shaded bars correspond to the bound form. See final sentence of the legend of Fig. 4 for details.

changes of ~80 mV. In c_3 II the only significant difference is in heme I, the one in contact with c_3 I in the complex, which changes ~20 mV. Therefore, as expected, the larger differences in each cytochrome are observed in the two interacting hemes. Upon complex formation, the contact regions of the two interacting proteins will experience a modification of their dielectric surroundings, changing from the high dielectric of the surrounding water, to the lower dielectric of the redox partner, which may affect considerably the redox potential of the hemes. Additionally, electrostatic interactions arising from close contact with charged groups from the partner may also have a noticeable effect.

Electron-proton coupling is common in this type of redox proteins, and was extensively characterized in previous experimental and theoretical works (Baptista et al., 1999; Coletta et al., 1991; Gayda et al., 1988; Louro et al., 2001a,b, 1997, 1996, 1998; Martel et al., 1999; Pereira et al., 2002; Salgueiro et al., 1997; Santos et al., 1984; Saraiva et al., 1998; Soares et al., 1997; Teixeira et al., 2002; Turner et al., 1994, 1996). This coupling is clearly present here, both in the free and complexed cytochromes c_3, as can be seen in Fig. 6. The change in the number of protons upon reduction is evident in the electrostatic potential interval in which the hemes titrate (Fig. 6, *A* and *B*). If we look at Fig. 6 *A*, the differences between the free and complex forms are much larger when the cytochrome is reduced (*left side of plot*), where the number of protons is lower in the free form. Almost no changes are observed between the two forms when the cytochrome is oxidized (*right side of plot*). On the other hand, in Fig. 6 *B*, we can see exactly the opposite behavior of that observed in Fig. 6 *A*. The number of protons

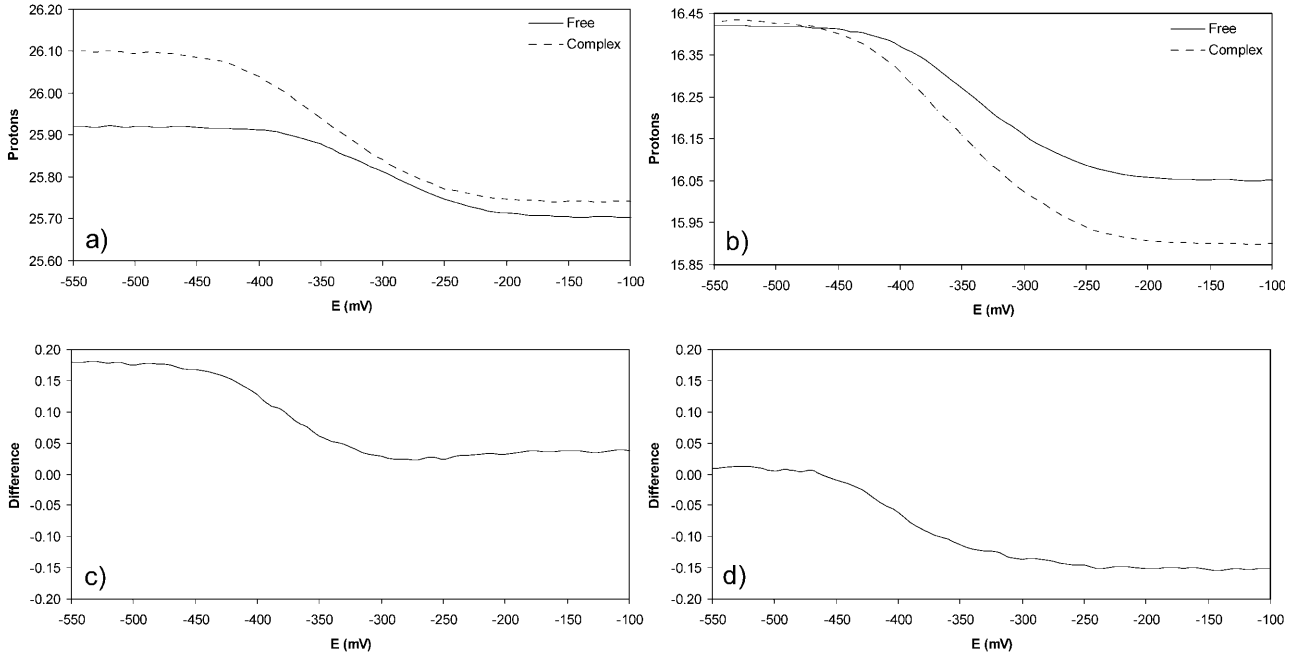

FIGURE 6 Variation in the number of protons in c_3 I (*A*) and c_3 II (*B*), with the solid lines corresponding to the free form and the dashed lines to the complex 2 form. Difference between the complex and the free forms (complex-free) in c_3 I (*C*) and c_3 II (*D*), respectively. See final sentence of the legend of Fig. 4 for details.

is almost the same, in the free and bound forms, when they are reduced (*left side of plot*), but in the oxidized form (*right side of plot*) the free cytochrome has more protons. These differences are not due to specific residues, but to a group of residues (data not shown). The change in the number of protons induced by complex formation can be seen more clearly using the difference between the complex and free forms, shown in Fig. 6, *C* and *D*. All these changes are small, with the largest change being ~0.18 proton units. Thus complex formation does not seem to have drastic effects in terms of proton capture/release, in the case studied here.

CONCLUSIONS

Various possible complexes for the molecular interaction between c_3 I and c_3 II from *Dv*H were obtained by rigid-body docking. The preferable regions of interaction for c_3 I are around hemes I and IV, and for c_3 II are around hemes I and III. Complex 1, corresponding to the lowest interaction energy (of the rigid-docking method), consists of an interaction between heme I from c_3 I and heme I from c_3 II. Complex 2, that corresponds to the second lowest interaction energy, consists of an interaction between heme IV from c_3 I and heme I from c_3 II. Complex formation, as judged from MD simulations with explicit water of both complexes, does not significantly change the conformation of the individual proteins, showing only small variations at the complex interface, relative to the free cytochromes. The stability of both complexes was further analyzed by binding free energy calculations using molecular mechanics, Poisson-Boltzmann, and surface accessibility methodologies. These calculations evidenced complex 2 as the most probable one for the interaction between these two proteins, showing that the rigid-body docking procedure used here is not good enough to energetically characterize the complexes formed in this case. As in other cases (Matias et al., 1999b, 2001), this interaction solution evidences the involvement of heme IV from c_3 I in the interaction with its physiological partners.

The reduction and protonation thermodynamics studies show that complex formation induces changes in the reduction potentials of the two cytochromes, especially in the hemes brought into contact (the largest change is observed in heme IV of c_3 I, that changes almost 80 mV). Overall, the two types of cytochromes c_3 respond in different ways to the presence of each other (in complex 2), with c_3 I decreasing its redox potential by ~36 mV and c_3 II by only 5 mV. These apparently small redox potential shifts induced by complex formation are crucial, however—giving rise to the thermodynamic release of electrons from c_3 I to c_3 II, following the physiologic direction of ET (Valente et al., 2001). This thermodynamic release can be important for ET kinetics, since as known from Marcus theory (and its further developments), these thermodynamic aspects are one of the determinant factors for ET kinetics.

The authors acknowledge helpful discussions with Prof. António V. Xavier, Dr. Ricardo Louro, and Dr. Inês C. Pereira.

Financial support from POCTI/BME/32789/99, SFRH/BD/6477/2001, and SFRH/BPD/5740/2001 are gratefully acknowledged.

REFERENCES

Baptista, A. M., P. J. Martel, and C. M. Soares. 1999. Simulation of electron-proton coupling with a Monte Carlo method: application to cytochrome c_3 using continuum electrostatics. *Biophys. J.* 76:2978–2998.

Baptista, A. M., and C. M. Soares. 2001. Some theoretical and computational aspects of the inclusion of proton isomerism in the protonation equilibrium of proteins. *J. Phys. Chem. B.* 105:293–309.

Barker, J. A., and R. O. Watts. 1973. Monte Carlo studies of the dielectric properties of water-like models. *Mol. Phys.* 26:789–792.

Bashford, D. 1997. An object-oriented programming suite for electrostatic effects in biological molecules. *In* Scientific Computing in Object-Oriented Parallel Environments, ISCOPE97. Y. Ishikawa, R. R. Oldehoeft, J. V. W. Reynders, and M. Tholburn, editors. Springer, Berlin, Germany. 233–240.

Bashford, D., and K. Gerwert. 1992. Electrostatic calculations of the pK_a values of ionizable groups in bacteriorhodopsin. *J. Mol. Biol.* 224: 473–486.

Bento, I., P. M. Matias, A. M. Baptista, P. N. da Costa, W. M. A. M. van Dongen, L. M. Saraiva, T. R. Schneider, C. M. Soares, and M. A. Carrondo. 2004. Molecular basis for redox-Bohr and cooperative effects in cytochrome c_3 from *Desulfovibrio desulfuricans* ATCC 27774: crystallographic and modelling studies of oxidised and reduced high resolution structures at pH 7.6. *Proteins.* 54:135–152.

Bento, I., V. H. Teixeira, A. M. Baptista, C. M. Soares, P. M. Matias, and M. A. Carrondo. 2003. Redox-Bohr and other cooperativity effects in the nine heme cytochrome *c* from *Desulfovibrio desulfuricans* ATCC 27774: crystallographic and modeling studies. *J. Biol. Chem.* 278:36455–36469.

Berendsen, H. J. C., J. P. M. Postma, W. F. van Gunsteren, A. DiNola, and J. R. Haak. 1984. Molecular dynamics with coupling to an external bath. *J. Chem. Phys.* 81:3684–3690.

Brennan, L., D. L. Turner, A. C. Messias, M. L. Teodoro, J. LeGall, H. Santos, and A. V. Xavier. 2000. Structural basis for the network of functional cooperativities in cytochrome c_3 from *Desulfovibrio gigas*: solution structure of the oxidized and reduced states. *J. Mol. Biol.* 298:61–82.

Bret, C., M. Roth, S. Norager, E. C. Hatchikian, and M. J. Field. 2002. Molecular dynamics study of *Desulfovibrio africanus* cytochrome c_3 in oxidized and reduced forms. *Biophys. J.* 83:3049–3065.

Burrows, A. L., L. H. Guo, A. O. Hill, G. McLendon, and F. Sherman. 1991. Direct electrochemistry of proteins: investigations of yeast cytochrome *c* mutants and their complex with cytochrome b_5. *Eur. J. Biochem.* 202:543–549.

Chothia, C. 1976. The nature of the accessible and buried surfaces in proteins. *J. Mol. Biol.* 105:1–14.

Coletta, M., T. Catarino, J. LeGall, and A. V. Xavier. 1991. A thermodynamic model for the cooperative functional properties of the tetraheme cytochrome c_3 from *Desulfovibrio gigas*. *Eur. J. Biochem.* 202:1101–1106.

Cunha, C. A., M. J. Romão, S. J. Sadeghi, E. Valetti, G. Gillardi, and C. M. Soares. 1999. Effects of protein-protein interactions on electron transfer: docking and electron transfer calculations for complexes between flavodoxin and *c*-type cytochromes. *J. Biol. Inorg. Chem.* 4:360–374.

Czjzek, M., F. Guerlesquin, M. Bruschi, and R. Haser. 1996. Crystal structure of a dimeric octaheme cytochrome c_3 (M_r 26000) from *Desulfovibrio desulfuricans* Norway. *Structure.* 4:395–404.

Czjzek, M., F. Payan, F. Guerlesquin, M. Bruschi, and R. Haser. 1994. Crystal structure of cytochrome c_3 from *Desulfovibrio desulfuricans* Norway at 1.7 Å resolution. *J. Mol. Biol.* 243:653–667.

Drepper, F., M. Hippler, W. Nitschke, and W. Haehnel. 1996. Binding dynamics and electron transfer between plastocyanin and photosystem I. *Biochemistry.* 35:1282–1295.

Einsle, O., S. Foerster, K. Mann, G. Fritz, A. Messerschmidt, and P. M. Kroneck. 2001. Spectroscopic investigation and determination of reactivity and structure of the tetraheme cytochrome c_3 from *Desulfovibrio desulfuricans* Essex 6. *Eur. J. Biochem.* 268:3028–3035.

Eisenhaber, F., and P. Argos. 1993. Improved strategy in analytic surface calculation for molecular systems: handling of singularities and computational efficiency. *J. Comp. Chem.* 14:1272–1280.

Eisenhaber, F., P. Lijnzaad, P. Argos, C. Sander, and M. Scharf. 1995. The double cubic lattice method: an efficient approach to numerical integration of surface area and volume and to dot surface contouring of molecular assemblies. *J. Comp. Chem.* 16:273–284.

Frazão, C., L. Sicker, G. Sheldrick, V. Lamzin, J. LeGall, and M. A. Carrondo. 1999. *Ab initio* structure solution of a dimeric cytochrome c_3 from *Desulfovibrio gigas* containing disulfide bridges. *J. Biol. Inorg. Chem.* 4:162–165.

Froloff, N., A. Windemuth, and B. Honig. 1997. On the calculation of binding free energies using continuum methods: application to MHC class I protein-peptide interactions. *Protein Sci.* 6:1293–1301.

Gayda, J., H. Benosman, P. Bertrand, C. More, and M. Asso. 1988. EPR Determination of interaction redox potentials in a multiheme cytochrome: cytochrome c_3 from *Desulfovibrio desulfuricans* Norway. *Eur. J. Biochem.* 177:199–206.

Gilson, M. K., J. A. Given, B. L. Bush, and J. A. McCammon. 1997. The statistical thermodynamic basis for computation of binding affinities: a critical review. *Biophys. J.* 72:1047–1069.

Gilson, M. K., and B. Honig. 1988. Calculation of the total electrostatic energy of a macromolecular system: solvation energies, binding energies, and conformational analysis. *Proteins Struct. Funct. Genet.* 4:7–18.

Goodsell, D. S., H. Lauble, C. D. Stout, and A. J. Olson. 1993. Automated docking in crystallography: analysis of the substrates of aconitase. *Proteins Struct. Funct. Genet.* 17:1–10.

Goodsell, D. S., and A. J. Olson. 1990. Automated docking of substrates to proteins by simulated annealing. *Proteins Struct. Funct. Genet.* 8: 195–202.

Harada, E., Y. Fukuoka, T. Ohmura, A. Fukunishi, G. Kawai, T. Fujiwara, and H. Akutsu. 2002. Redox-couple conformational alternations in cytochrome c_3 from *D. vulgaris* Miyazaki F on the basis of its reduced solution structure. *J. Mol. Biol.* 319:767–778.

Haser, R., M. Pierrot, P. M. Frey, F. Payan, and J. P. Astier. 1979. Structure and sequence of the multihaem cytochrome c_3. *Nature.* 282:806–810.

Hermans, J., H. J. C. Berendsen, W. F. van Gunsteren, and J. P. M. Postma. 1984. A consistent empirical potential for water-protein interactions. *Biopolymers.* 23:1513–1518.

Higuchi, Y., M. Kusunoki, Y. Matsuura, N. Yasuoka, and M. Kakudo. 1984. Refined structure of cytochrome c_3 at 1.8 Å resolution. *J. Mol. Biol.* 172:109–139.

Kraulis, P. J. 1991. MOLSCRIPT: a program to produce both detailed and schematic plots of proteins structures. *J. Appl. Crystallogr.* 24:946–950.

Kuhn, B., and P. A. Kollman. 2000. A ligand that is predicted to bind better to avidin than biotin: insights from computational fluorine scanning. *J. Am. Chem. Soc.* 122:3909–3916.

Laskowski, A., M. MacArthur, D. Moss, and J. Thorton. 1993. PROCHECK: a program to check the stereochemical quality of protein structures. *J. Appl. Crystallogr.* 26:283–291.

Louro, R. O., I. Bento, P. M. Matias, T. Catarino, A. M. Baptista, C. M. Soares, M. A. Carrondo, D. L. Turner, and A. V. Xavier. 2001a. Conformational component in the coupled transfer of multiple electrons and protons in a monomeric tetrahaem cytochrome. *J. Biol. Chem.* 276:44044–44051.

Louro, R. O., T. Catarino, J. LeGall, D. L. Turner, and A. V. Xavier. 2001b. Cooperativity between electrons and protons in a monomeric cytochrome c_3: the importance of mechanochemical coupling for energy transduction. *Chem. Biochem.* 2:831–837.

Louro, R. O., T. Catarino, J. LeGall, and A. V. Xavier. 1997. Redox-Bohr effect in electron/proton energy transduction: cytochrome c_3 coupled to hydrogenase works as a ''proton thruster'' in *Desulfovibrio vulgaris. J. Biol. Inorg. Chem.* 2:488–491.

Louro, R. O., T. Catarino, C. A. Salgueiro, J. LeGall, and A. V. Xavier. 1996. Redox-Bohr effect in the tetrahaem cytochrome c_3 from *Desulfovibrio vulgaris*: a model for energy transduction mechanisms. *J. Biol. Inorg. Chem.* 1:34–38.

Louro, R. O., T. Catarino, D. L. Turner, M. A. Piçarra-Pereira, I. Pacheco, J. LeGall, and A. V. Xavier. 1998. Functional and mechanistic studies of cytochrome c_3 from *Desulfovibrio gigas*—thermodynamics of a ''proton-thruster.'' *Biochemistry.* 37:15808–15815.

Magro V., L. Pieulle, N. Forget, B. Guigliarelli, Y. Petillot, and E. C. Hatchikian. 1997. Further characterization of the two tetraheme cytochrome c_3 from *Desulfovibrio africanus*: nucleotide sequences, EPR spectroscopy and biological activity. *Biochim. Biophys. Acta.* 1342:149–163.

Marcus, R. A., and N. Sutin. 1985. Electron transfers in chemistry and biology. *Biochim. Biophys. Acta.* 811:265–322.

Martel, P. J., C. M. Soares, A. M. Baptista, M. Fuxreiter, G. Náray-Szabó, R. O. Louro, and M. A. Carrondo. 1999. Comparative redox and pK_a calculations on cytochrome c_3 from several *Desulfovibrio* species using continuous electrostatic methods. *J. Biol. Inorg. Chem.* 4:73–86.

Martí-Renom, M. A., A. C. Stuart, A. Fiser, R. Sánches, F. Melo, and A. Sali. 2000. Comparative protein structure modeling of genes and genomes. *Annu. Rev. Biophys. Biomol. Struct.* 29:291–325.

Matias, P. M., R. Coelho, I. A. C. Pereira, A. V. Coelho, A. W. Thompson, L. C. Sieker, J. LeGall, and M. A. Carrondo. 1999a. The primary and three-dimensional structures of a nine-haem cytochrome *c* from *Desulfovibrio desulfuricans* ATCC 27774 reveal a new member of the HMC family. *Structure.* 7:119–130.

Matias, P. M., C. Frazão, J. Morais, M. Coll, and M. A. Carrondo. 1993. Structure analysis of cytochrome c_3 from *Desulfovibrio vulgaris* Hildenborough at 1.9 Å resolution. *J. Mol. Biol.* 234:680–699.

Matias, P. M., J. Morais, R. Coelho, M. A. Carrondo, K. Wilson, Z. Dauter, and L. Sieker. 1996. Cytochrome c_3 from *Desulfovibrio gigas*: crystal structure at 1.8 Å resolution and evidence for a specific calcium-binding site. *Protein Sci.* 5:1342–1354.

Matias, P. M., L. M. Saraiva, C. M. Soares, A. V. Coelho, J. LeGall, and M. A. Carrondo. 1999b. Nine-haem cytochrome *c* from *Desulfovibrio desulfuricans* ATCC 27774: primary sequence determination, crystallographic refinement at 1.8 Å and modeling studies of its interaction with the tetrahaem cytochrome c_3. *J. Biol. Inorg. Chem.* 4:478–494.

Matias, P. M., C. M. Soares, L. M. Saraiva, R. Coelho, J. Morais, J. LeGall, and M. A. Carrondo. 2001. [NiFe] Hydrogenase from *Desulfovibrio desulfuricans* ATCC 27774: primary sequence determination, crystallographic refinement at 1.8 Å and modeling studies of its interaction with the tetra-haem cytochrome c_3. *J. Biol. Inorg. Chem.* 6:63–81.

Merrit, E. A., and D. J. Bacon. 1997. Raster3D photorealistic molecular graphics. *Methods Enzymol.* 277:505–524.

Messias, A. C., D. H. W. Kastrau, H. S. Costa, J. LeGall, D. L. Turner, H. Santos, and A. V. Xavier. 1998. Solution structure of *Desulfovibrio vulgaris* (Hildenborough) ferrocytochrome c_3: structural basis for functional cooperativity. *J. Mol. Biol.* 281:719–739.

Mizuguchi, K., C. M. Deane, T. L. Blundell, and J. P. Overington. 1998. HOMSTRAD: a database of protein structure alignments for homologous families. *Protein Sci.* 7:2469–2471.

Moore, G. R. 1996. Haemoproteins. *In* Protein Electron Transfer. D. S. Bendall, editor. BIOS Scientific Publishers Ltd., Oxford, UK. 189–216.

Moore, G. R., G. W. Pettigrew, and N. K. Rogers. 1986. Factors influencing redox potentials of electron transfer proteins. *Proc. Natl. Acad. Sci. USA.* 83:4998–4999.

Morais, J., P. N. Palma, C. Frazão, J. Caldeira, J. LeGall, I. Moura, J. J. G. Moura, and M. A. Carrondo. 1995. Structure of the tetraheme cytochrome from *Desulfovibrio desulfuricans* ATCC 27774: x-ray diffraction and electron paramagnetic resonance studies. *Biochemistry.* 34:12830–12841.

Norager, S., P. Legrand, L. Pieulle, C. Hatchikian, and M. Roth. 1999. Crystal structure of the oxidized and reduced acidic cytochrome c_3 from *Desulfovibrio africanus*. *J. Mol. Biol.* 298:881–902.

Papa, S., F. Guerrieri, and G. Izzo. 1979. Redox-Bohr effects in the cytochrome system of mitochondria. *FEBS Lett.* 105:213–216.

Pereira, I. A. C., C. V. Romão, A. V. Xavier, J. LeGall, and M. Teixeira. 1998. Electron transfer between hydrogenases and mono and multiheme cytochromes in *Desulfovibrio* ssp. *J. Biol. Inorg. Chem.* 3:494–498.

Pereira, P. M., I. Pacheco, D. L. Turner, and R. O. Louro. 2002. Structure-function relationship in type II cytochrome c_3 from *Desulfovibrio africanus*: a novel function in a familiar heme core. *J. Biol. Inorg. Chem.* 7:815–822.

Pickett, S. D., and M. J. E. Sternberg. 1993. Empirical scale of side-chain conformational entropy in protein folding. *J. Mol. Biol.* 231:825–839.

Pieulle, L., J. Haladjian, J. Bonicel, and E. C. Hatchikian. 1996. Biochemical studies of the c-type cytochromes of the sulfate reducer *Desulfovibrio africanus*. Characterization of two tetraheme cytochromes c_3 with different specificity. *Biochim. Biophys. Acta.* 1273:51–61.

Rees, D. C. 1985. Electrostatic influence on energetics of electron transfer reactions. *Proc. Natl. Acad. Sci. USA.* 82:3082–3085.

Ryckaert, J.-P., G. Ciccotti, and H. J. C. Berendsen. 1977. Numerical integration of the Cartesian equations of motion of a system with constraints: molecular dynamics of *n*-alkanes. *J. Comp. Phys.* 23: 327–341.

Salgueiro, C. A., D. L. Turner, J. LeGall, and A. V. Xavier. 1997. Reevaluation of the redox and redox-Bohr cooperativity in tetrahaem *Desulfovibrio vulgaris* (Miyazaki F) cytochrome c_3. *J. Biol. Inorg. Chem.* 2:343–349.

Sali, A., and T. L. Blundell. 1993. Comparative protein modelling by satisfaction of spatial restraints. *J. Mol. Biol.* 234:779–815.

Sánchez, R., and A. Sali. 1997. Advances in comparative protein-structure modelling. *Curr. Opin. Struct. Biol.* 7:206–214.

Santos, H., J. J. G. Moura, I. Moura, J. LeGall, and A. V. Xavier. 1984. NMR studies of electron transfer mechanism in a protein with interacting redox centers: *Desulfovibrio gigas* cytochrome c_3. *Eur. J. Biochem.* 141:283–296.

Saraiva, L. M., C. A. Salgueiro, P. N. Costa, A. C. Messias, J. LeGall, W. M. A. M. van Dongen, and A. V. Xavier. 1998. Replacement of Lysine 45 by uncharged residues modulates the redox-Bohr effect in tetraheme cytochrome c_3 of *Desulfovibrio vulgaris* (Hildenborough). *Biochemistry.* 37:12160–12165.

Scott, W. R. P., P. H. Hünenberger, I. G. Tironi, A. E. Mark, S. R. Billeter, J. Fennen, A. E. Torda, T. Huber, P. Krüger, and W. F. van Gunsteren. 1999. The GROMOS biomolecular simulation program package. *J. Phys. Chem. A.* 103:3596–3607.

Simões, P., P. M. Matias, J. Morais, K. Wilson, Z. Dauter, and M. A. Carrondo. 1998. Refinement of the three-dimensional structures of cytochrome c_3 from *Desulfovibrio vulgaris* Hildenborough at 1.67 Å resolution and from *Desulfovibrio desulfuricans* ATCC 27774 at 1.6 Å resolution. *Inorg. Chim. Acta.* 273:213–224.

Sitkoff, D., K. A. Sharp, and B. Honig. 1994. Accurate calculations of hydration free energies using macroscopic solvent models. *J. Phys. Chem.* 98:1978–1988.

Smith, K. C., and B. Honig. 1994. Evaluation of the conformational free energies of loops in proteins. *Proteins Struct. Funct. Genet.* 18:119–132.

Soares, C. M., P. J. Martel, and M. A. Carrondo. 1997. Theoretical studies on the redox-Bohr effect in cytochrome c_3 from *Desulfovibrio vulgaris* Hildenborough. *J. Biol. Inorg. Chem.* 2:714–727.

Soares, C. M., P. J. Martel, J. Mendes, and M. A. Carrondo. 1998. Molecular dynamics simulation of cytochrome c_3: studying the reduction processes using free energy calculations. *Biophys. J.* 74:1708–1721.

Soriano, G. M., W. A. Cramer, and L. I. Krishtalik. 1997. Electrostatic effects on electron-transfer kinetics in the cytochrome *f*-plastocyanin complex. *Biophys. J.* 73:3265–3276.

Teixeira, V. H., C. M. Soares, and A. M. Baptista. 2002. Studies of the reduction and protonation behavior of the tetraheme cytochromes using atomic detail. *J. Biol. Inorg. Chem.* 7:200–216.

Tironi, I. G., R. Sperb, P. E. Smith, and W. F. van Gunsteren. 1995. A generalized reaction field method for molecular dynamics simulations. *J. Chem. Phys.* 102:5451–5459.

Turner, D. L., C. A. Salgueiro, T. Catarino, J. LeGall, and A. V. Xavier. 1994. Homotropic and heterotropic cooperativity in the tetrahaem cytochrome c_3 from *Desulfovibrio vulgaris*. *Biochim. Biophys. Acta.* 1187:232–235.

Turner, D. L., C. A. Salgueiro, T. Catarino, J. LeGall, and A. V. Xavier. 1996. NMR studies of cooperativity in the tetrahaem cytochrome c_3 from *Desulfovibrio vulgaris*. *Eur. J. Biochem.* 241:723–731.

Valente, F. M. A., L. M. Saraiva, J. LeGall, A. V. Xavier, M. Teixeira, and I. A. C. Pereira. 2001. A membrane-bound cytochrome c_3: a type II cytochrome c_3 from *Desulfovibrio vulgaris* Hildenborough. *Chem. Biochem.* 2:895–905.

van Gunsteren, W. F., and H. J. C. Berendsen. 1990. Computer simulation of molecular dynamics: methodology, applications and perspectives in chemistry. *Angew. Chem. Int.* 29:992–1023.

van Gunsteren, W. F., S. R. Billeter, A. A. Eising, P. H. Hunenberger, P. Kruger, A. E. Mark, W. R. P. Scott, and I. G. Tironi. 1996. Biomolecular Simulation: The GROMOS96 Manual and User Guide. BIOMOS b.v. Groningen, Zurich, Switzerland.

Vanderkooi, J., and M. Erecinska. 1974. Cytochrome *c* interaction with membranes: interaction of cytochrome *c* with isolated membrane fragments and purified enzymes. *Arch. Biochem. Biophys.* 162:385–391.

Warshel, A. 1982. Dynamics of reactions in polar solvents. Semiclassical trajectory studies of electron-transfer and proton-transfer reactions. *J. Phys. Chem.* 86:2218–2224.

Xavier, A. V. editor. 1985. Frontiers in Bioinorganic Chemistry. VCH Publishers, Weinheim, Germany.

Yagi, T., M. Honya, and N. Tamiya. 1968. Purification and properties of hydrogenases of different origins. *Biochim. Biophys. Acta.* 153:699–705.

Zhang, H., C. J. Carrell, D. Huang, V. Sled, T. Ohnishi, J. L. Smith, and W. A. Cramer. 1996. Characterization and crystallization of the lumen side domain of the chloroplast Rieske iron-sulfur protein. *J. Biol. Chem.* 271:31360–31366.

Zhou, H. 1994. Effects of mutations and complex formation on the reduction potentials of cytochrome *c* and cytochrome *c* peroxidase. *J. Am. Chem. Soc.* 116:10362–10375.

Zhu, Z., L. M. Cunane, Z. Chen, R. C. E. Durley, F. S. Mathews, and V. L. Davidson. 1998. Molecular basis for interprotein complex-dependent effects on the redox properties of amicyanin. *Biochemistry.* 37:17128–17136.